

Heavy-ion irradiation of UBe superconductors

H.A. Radovan, E. Behne, R.J. Zieve
Physics Department, University of California at Davis

J.S. Kim, G.R. Stewart
Physics Department, University of Florida

W.-K. Kwok
Argonne National Laboratory, Division of Materials Science

R.D. Field
Los Alamos National Laboratory

We irradiate the heavy fermion superconductors $(U, Th)Be_{13}$ with high-energy heavy ions. Damage from the ions affects both heat capacity and magnetization measurements, although much less dramatically than in other superconductors. From these data and from direct imaging, we conclude that the irradiation does not create the amorphous columnar defects observed in high-temperature superconductors and other materials. We also find that the damage suppresses the two superconducting transitions of $U_{0.97}Th_{0.03}Be_{13}$ by comparable amounts, unlike their response to other types of defects.

PACS numbers: 74.70.Tx, 61.80.Jh

I. INTRODUCTION

Microscopic lattice disorder can have interesting effects, particularly on unconventional superconductors. Sensitivity of the critical temperature T_c to non-magnetic scatterers serves as evidence of non- s -wave electron-pairing. Defects can be introduced during sample fabrication, or induced afterwards by irradiation. The latter possibility encompasses both point defects created by light ions and other particles, and amorphous columns created by high-energy heavy ions. These columnar defects, which have been heavily studied in high-temperature superconductors (HTS), serve as highly efficient pinning centers for vortices and alter a sample's response to a magnetic field.

Little work has been done on another group of unconventional superconductors, the heavy fermion (HF) systems. The two orders of magnitude difference in the critical temperatures of HTS and HF superconductors changes the scale for thermal effects. Thermal fluctuations which complicate HTS behavior should be absent in HF.

The spectacular response of one heavy fermion material, UBe_{13} , to thorium doping makes it a good candidate for investigating other forms of lattice disorder. $T_c(x)$ is not monotonic for $U_{1-x}Th_xBe_{13}$, and a second thermodynamic phase transition appears for $0.019 < x < 0.043$ [1, 2]. No other dopant has such effects. The Be as well as the U is sensitive to substitution details. The superconducting transition is suppressed below 0.015 K for $UBe_{12.94}Cu_{0.06}$ [3], while the same amount of B has virtually no effect [4].

Multiple superconducting phases indicate an unconventional order parameter. A second HF material, UPt_3 , also exhibits a double transition [5]. Furthermore, the lower phases of both UPt_3 and $U_{1-x}Th_xBe_{13}$ have a significantly reduced vortex relaxation rate, while in pure UBe_{13} the relaxation rate is linear in temperature [6]. This may be evidence of time re-

versal symmetry breaking in the lower phase. If time reversal symmetry is broken, spontaneous magnetic fields can appear. Boundaries between different magnetic domains can obstruct vortex motion, leading to the observed drop in relaxation rate. Vortex motion is also reduced in $U_{1-x}Th_xBe_{13}$ for zero-field-cooling as compared to the field-cooling case [7]. Domain wall pinning may explain this effect as well, since cooling in a field should lead to larger domains and fewer domain walls. The atypical vortex behavior and the distinction between the two superconducting phases suggests that vortices may also have interesting interactions with other types of pin sites, such as columnar defects.

Here we investigate heavy-ion irradiation of $(U, Th)Be_{13}$. We show that calculations predict columnar tracks to form. However, heat capacity measurements, imaging, and magnetization measurements suggest that such tracks are not actually present. We also discuss how heavy-ion damage affects the different superconducting phases.

II. IRRADIATION DAMAGE

The thermal spike model explains damage creation in both elements and alloys [8, 9, 10]. In this model, the heavy ion loses energy primarily to the electrons, which in turn excite phonons. The electron-phonon coupling strength g determines how fast the energy is transferred to the lattice, while the thermal conductivities κ_e and κ_p of electrons and phonons govern how the energy spreads through the sample. The coupled differential equations

$$C_e \frac{\partial T_e}{\partial t} = \frac{\partial}{\partial r} (\kappa_e \frac{\partial T_e}{\partial r}) + \frac{\kappa_e}{r} \frac{\partial T_e}{\partial r} - g(T_e - T_p) + A(r, t)$$

TABLE I: Parameters for thermal spike calculations in UBe₁₃.

Debye temperature, Θ_D	620 K	[12]
Melting temperature, T_m	2273 K	[13]
Resistivity, ρ	$110 \mu\Omega\text{-cm}$ at 300 K	[14]
Atomic density, n_a	$1 \times 10^{23}/\text{cm}^3$	[15]
Valence, z	2.1	
C_e	$4.3 \times 10^3 \text{ erg}/\text{cm}^3 \text{ K}$	
C_p	$4.1 \times 10^3 \text{ erg}/\text{cm}^3 \text{ K}$	
κ_e	$2.2 \times 10^3 T \text{ erg}/\text{cm K}$	
κ_p	$9.9 \times 10^7/T \text{ erg}/\text{cm K}$	[16]

$$C_p \frac{\partial T_p}{\partial t} = \frac{\partial}{\partial r} (\kappa_p \frac{\partial T_p}{\partial r}) + \frac{\kappa_p}{r} \frac{\partial T_p}{\partial r} + g(T_e - T_p)$$

describe the energy transfer. Here κ_e and the specific heat C_e of the electron system are functions of the electron temperature T_e , while κ_p and the lattice specific heat C_p depend on the phonon temperature T_p . $S_e = -\frac{dE}{dx}|_e$ is the energy loss from the heavy ion to the electrons in the target. As S_e increases, a threshold value allows formation of amorphous tracks. With further increase the track radius grows. For the radial distribution of the original ion energy loss we use

$$A(r, t) \propto \frac{1}{r} \left[\frac{(1 - \frac{r+\theta}{r_{max}+\theta})^{0.927}}{r + \theta} \right] \times [1 + \frac{K(r-L)}{M} e^{-(r-L)/M}] e^{-(t-t_o)^2/2t_o^2},$$

as in [11]. Here $K = 19\beta^{1/3}$, $L = 0.1 \text{ nm}$, $M = (1.5 + 0.5\beta) \text{ nm}$, and β is the ion velocity relative to the speed of light. The maximum range $r_{max} = 6 \times 10^{-6} \left(\frac{2mc^2\beta^2}{1-\beta^2} \right)^{1.079} \text{ cm}$, where m is the electron mass in grams and c the speed of light in cm/s. The time t_o is of order 10^{-15} s and $\theta = 9.84 \times 10^{-9} \text{ cm}$. The normalization of $A(r, t)$ is chosen so that the total energy transfer to the electrons equals S_e . This formula, particularly the term involving K , L , and M , comes from fits to observed radiation distributions in water [11]. Thermal spike calculations using these equations successfully predict the existence and even radius of columnar defects in a variety of pure metals and alloys [8].

Numerical solution of these equations requires knowledge of various parameters of the material. Table I shows the values we use. Since most of the simulation is at high temperature, we use high-temperature limits in several cases. The electronic and lattice specific heats are $C_e = 1.5k_Bn_e$ and $C_p = 3k_Bn_a$. The density of atoms in the lattice is n_a , while the electron density is $n_e = zn_a$ with z the average valence of the atoms composing the material. For the electronic thermal conductivity κ_e we use the Wiedemann-Franz law. Although in most metals the high-temperature electrical resistivity is proportional to temperature, in UBe₁₃ the resistivity is nearly constant, so κ_p is itself proportional to temperature [14]. For the lattice thermal conductivity κ_e we expect a $1/T$ temperature dependence and obtain the prefactor from the 90 K value [16].

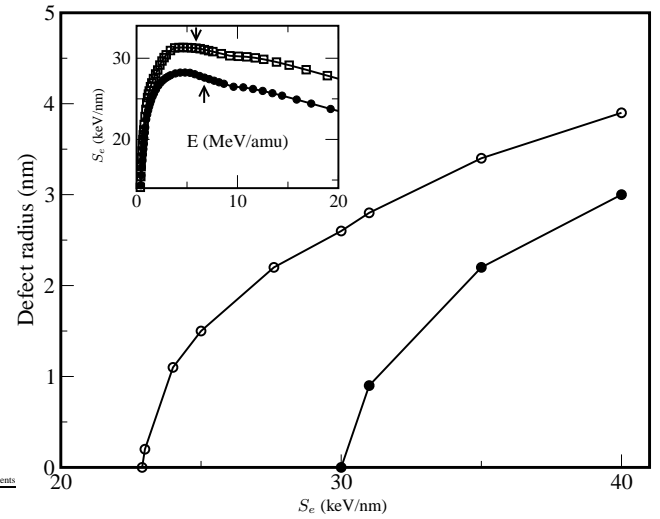


FIG. 1: Predicted defect radius in UBe₁₃. The two curves use heat of fusion $2 \times 10^{10} \text{ erg}/\text{cm}^3$ (●) and $4 \times 10^{10} \text{ erg}/\text{cm}^3$ (○). Inset: SRIM simulation of electronic energy loss for $^{238}\text{U}^{67+}$ (□) and $^{208}\text{Pb}^{56+}$ (●) ions in UBe₁₃. The arrows indicate the energy of the beams used for our irradiations.

The heat of fusion of a compound equals the latent heat of its component elements, plus the difference between the liquid state mixing enthalpy and the solid enthalpy of formation. Typical values are 10^{10} to $10^{11} \text{ erg}/\text{cm}^3$. In this case the U and Be latent heats contribute $2 \times 10^{10} \text{ erg}/\text{cm}^3$. The heat of formation at room temperature is $-2 \times 10^{10} \text{ erg}/\text{cm}^3$ [13], so $4 \times 10^{10} \text{ erg}/\text{cm}^3$ is an upper bound on the heat of fusion. Although the mixing enthalpy is unknown, $2 \times 10^{10} \text{ erg}/\text{cm}^3$ might be a more reasonable estimate for the heat of fusion.

Finally, for the electron-phonon coupling we use [8]

$$g = \frac{\pi^4 k_B^4 n_e^2 \Theta_D^2 \rho}{18L\hbar^2 (6\pi^2 n_a)^{2/3}} \frac{1}{T_e}.$$

Here $L = 0.245 \text{ erg}\cdot\Omega/\text{K}$ is the Lorentz number.

Figure 1 shows the defect radius obtained by solving the thermal spike equations numerically. With resistivity, Debye temperature, and heat of formation similar to those of Ce and Y alloys studied earlier, the key difference in UBe₁₃ appears to be its high atomic density, which makes it particularly sensitive to irradiation. The unusual temperature independence of the resistivity tends only to decrease the sensitivity to defect formation.

III. SAMPLE PREPARATION

Our samples are polycrystalline UBe₁₃ and U_{0.97}Th_{0.03}Be₁₃ pieces with a grain size of about 100 μm , prepared by arc melting in an argon atmosphere and subsequent annealing at 1400° C in a beryllium atmosphere for 1000 hours [17]. Before irradiation, samples are thinned to 25 μm to prevent ion implantation, with a typical lateral

TABLE II: Effects of irradiation on transitions in (U,Th)Be₁₃.

	T_c (0 T)	T_c (3 T)	T_c (5 T)	T_c (7 T)	% change at 7 T
UBe ₁₃	770		750	715*	-7.1
U _{0.97} Th _{0.03} Be ₁₃ (T_{c1})	625	620*	613	530	-15.2
U _{0.97} Th _{0.03} Be ₁₃ (T_{c2})	412		400	345	-16.3

Transition temperatures marked by (*) come from magnetization measurements, the remainder from heat capacity.

TABLE III: Effects of irradiation on transitions in YBa₂Cu₃O_{7-x}.

T_c suppression	Density	Ion	E (MeV/amu)	S_e (keV/nm)	Source
5.3%	2T	U	4.2	14.6	[20]
3.9%	1T	Sn	6.2	16.6	[21]
0.3%	2T	Pb	26.9	20.3	[22]
0.3%	2T	Au	19.8	21.1	[23]

dimension of 1 mm. The irradiation is performed at ATLAS, Argonne National Laboratory with 1.4 GeV $^{238}\text{U}^{67+}$ and $^{208}\text{Pb}^{56+}$ ions. The ion velocities are 5.9 MeV/amu and 6.7 MeV/amu, respectively. The matching fields B_Φ , at which the vortex density and track density are equal, range from 0.1 T and 7 T, corresponding to typical lateral track separations from 155 to 18.5 nm. The $^{208}\text{Pb}^{56+}$ ions were used for the 3 T and 7 T samples, while the $^{238}\text{U}^{67+}$ were used for the remaining samples. The irradiation takes up to two hours, depending on dosage. Because of the very small probability that two ions will reach the sample at nearly the same time and position, we assume that each ion acts independently in damaging the sample.

The inset of Figure 1 shows the electronic energy loss S_e as a function of the incident beam energy, obtained from a Stopping and Range of Ions in Matter (SRIM-98 code [18]) simulation. The beam energy used for the irradiation is near the maximum and gives $S_e = 31.2$ keV/nm for uranium, $S_e = 27.6$ keV/nm for lead. The corresponding nuclear energy losses are negligible, 0.05 keV/nm and 0.04 keV/nm, respectively. The predicted stopping distances are 56 μm and 60 μm , more than twice the sample thickness. From our thermal spike calculation, the irradiation should produce defects with radius 2.8 nm (uranium) or 2.2 nm (lead).

IV. T_c SUPPRESSION

We measure heat capacity on a dilution refrigerator at temperatures down to 100 mK and magnetic fields up to 8 Tesla. We use a relaxation method with a RuO₂ thin film thermometer, a [50:50] AuCr thin film heater, and a fine copper wire as a heat link.

Figure 2 shows C/T for the unirradiated, 5 T, and 7 T U_{0.97}Th_{0.03}Be₁₃ samples. Since we do not know the precise sample sizes, we use a multiplicative constant to set the normal state value of C/T to 1.1 J/mole K² for each curve. We do not adjust the measured heat capacity for any contribution from the thermometer, heater, or mount; but comparing the curves shown to previous heat capacity measurements on bulk

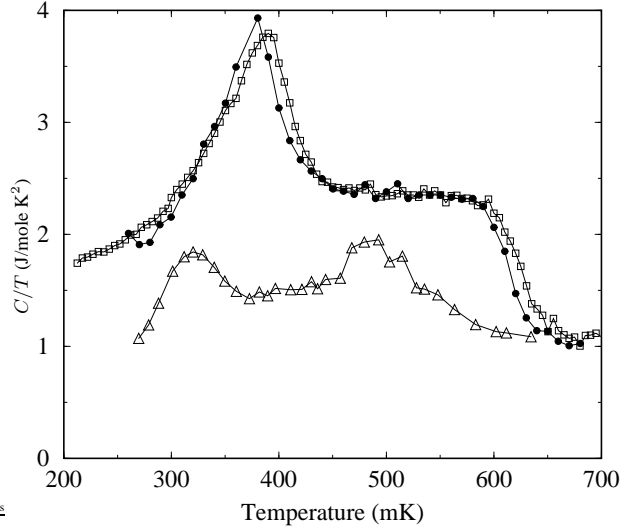


FIG. 2: Zero-field heat capacity of unirradiated (\square), 5 T irradiated (\bullet), and 7 T irradiated (Δ) U_{0.97}Th_{0.03}Be₁₃.

samples suggests that background effects are less than 30% of our signal. In any case, the background should not affect our determination of the T_c suppression or transition width.

Irradiation does not measurably change T_c up to $B_\Phi = 2$ T. As shown in Figure 2 for U_{0.97}Th_{0.03}Be₁₃, C/T changes shape only slightly even at a defect density of 5 T, broadening by several mK [19]. At the higher defect density of $B_\Phi = 7$ T, the transitions do change shape. The upper transition widens by roughly a factor of two, and both decrease significantly in amplitude. Here width is defined by identifying the change in C/T across the transition and using the temperature difference between the 10% and 90% values of the heat capacity. Irradiation has a similar effect on pure UBe₁₃, reducing T_c and slightly broadening the transition, while retaining the shape of the C/T curve up to 5 T. Table II summarizes the effects of irradiation on transition temperatures for both compounds. The

marked transitions come from magnetization measurements rather than heat capacity, as will be discussed later.

Since the $^{208}\text{Pb}^{56+}$ ions used for irradiation have less energy loss than the $^{238}\text{U}^{67+}$ ions, they produce smaller defects in a thermal spike calculation. Depending on the value of the heat of formation, the uranium atoms might even produce defects while the lead atoms do not. We note here that the T_c depression for the 3 T sample is consistent with the others. The 7 T samples have, if anything, a larger change in T_c than expected from the lower irradiation dosages. Thus it appears that the $^{208}\text{Pb}^{56+}$ ions are do much damage as the $^{238}\text{U}^{67+}$ ions, despite their smaller energy loss.

It is tempting to take the nearly identical percentage suppression of the two thoriated transitions as evidence that both superconducting phases have the same pairing symmetry. However, the lower transition is between two superconducting phases, rather than between a superconducting and a normal phase. The usual arguments on how impurities affect the transition do not apply. We do note that the heavy-ion irradiation produces a different response than either non-magnetic or magnetic substitutional impurities [24]. Non-magnetic (La) impurities depress the upper transition but leave the lower transition unchanged, while magnetic (Gd) impurities suppress the lower transition more than twice as strongly as the upper one [24]. These contrasting behaviors of the two transitions for different types of defects emphasize the extreme sensitivity of the (U,Th)Be₁₃ system to changes in electronic structure.

For comparison Table III shows data on T_c -reduction by columnar defects in YBa₂Cu₃O_{7-x} crystals. The smaller T_c reduction at high energy than at lower energy may occur because faster ions deposit their energy over a larger transverse distance. Since the energy heats a larger region, the center of the track is less likely to reach the melting temperature. Our irradiation energies are near the lower values that produce more damage. Yet the 5.3% reduction found at 2 T for U ions in YBa₂Cu₃O_{7-x} is larger even than the reduction we find at 5 T in (U,Th)Be₁₃.

By contrast with our modest T_c reduction, point defects from neutron or light-ion irradiation reduce T_c more sharply in HF superconductors than in any other superconductors [3, 25]. At an estimated 1% of atoms displaced, the superconducting transition temperature of UPt₃ is suppressed by 60%, while a similar radiation flux in UBe₁₃ reduces T_c by 40% [3]. If we take the expected 3 nm defect radius for our samples, and a typical defect spacing of 32 nm (corresponding to $B_\phi = 2$ Tesla), we estimate that about 3% of the atoms lie within the melted region. Since our defects are localized in columns, as opposed to being evenly distributed in samples irradiated with lighter particles, we do not expect identical T_c suppression in the two cases. However, qualitatively the lack of T_c reductions in our samples is striking; even our $B_\phi = 7$ Tesla irradiation affects T_c far less than the point defect work.

V. IMAGING

After irradiation, both the 2.0 T UBe₁₃ and 7.0 T U_{0.97}Th_{0.03}Be₁₃ crystals were further thinned and viewed in both a Philips CM-30 transmission electron microscope (TEM) and a JEOL 3000F high resolution transmission electron microscope. The planes used for the images on the JEOL machine limited the resolution to about 0.5 nm. At $B_\Phi = 2.0$ T the defects should be about 32 nm apart. The total viewing area of about 73,000 nm² should contain about 70 defects but in fact shows no evidence of amorphous columns. For the 7.0 T sample, the imaging area of over 54,000 nm² should have nearly 200 defects. We again find no damage of radius greater than 2 nm, and only six candidates with radius from 1 nm to 2 nm. Of these, closer examination shows that three are edge dislocations. The remaining candidates could also be dislocations, viewed from angles that do not clearly show a lattice plane ending. We find no compelling reason to identify them with columnar tracks, since they do not match the expected defects either in size or in density. We conclude that columnar defects are either absent in our sample or far smaller than anticipated from our thermal spike model calculations. This is consistent with the small change in T_c compared to other irradiated heavy fermion materials.

We emphasize that the microscopes we used *can* detect amorphous regions of the expected size. A transmission electron microscope successfully imaged columnar defects of radius 5 nm in UO₂ [26]. High resolution TEM has detected columnar defects with radius down to 1 nm, for example in tin oxide [27] and Bi₂Sr₂CaCu₂O_{8+δ} [28].

VI. MAGNETIZATION MEASUREMENTS

For magnetic measurements we use bismuth Hall probes with active area $10 \times 15 \mu\text{m}^2$. We place the sample flat atop the substrate for the Hall probe. The probe measures total field at a spot near the surface of the sample, from which we extract the local magnetization of the superconductor. We typically ramp the applied magnetic field at 15 gauss per minute, and take hysteresis loops large enough to allow for full penetration. The width of the hysteresis loop, ΔM , is proportional to the critical current j_c ; and we measure both its temperature and its field dependence.

Figure 3 compares hysteresis loop width and heat capacity for the crystal. As T increases, the hysteresis loop width decreases, closing at the same superconducting T_c measured with heat capacity. For the 3 T thoriated and 7 T pure samples, the T_c values in Table II are determined from magnetization rather than heat capacity data.

The loop width varies from a few gauss to 64 gauss at 200 mK. In a simple Bean model, the magnetization steadily increases on moving from the outside towards the center of the sample. Our Hall probes, which measure local magnetization, are positioned near the center of the sample. Thus we expect larger hysteresis loop widths for larger samples. In practice, we do find positive correlation between sample size and loop width, but other factors play major roles as well. The width

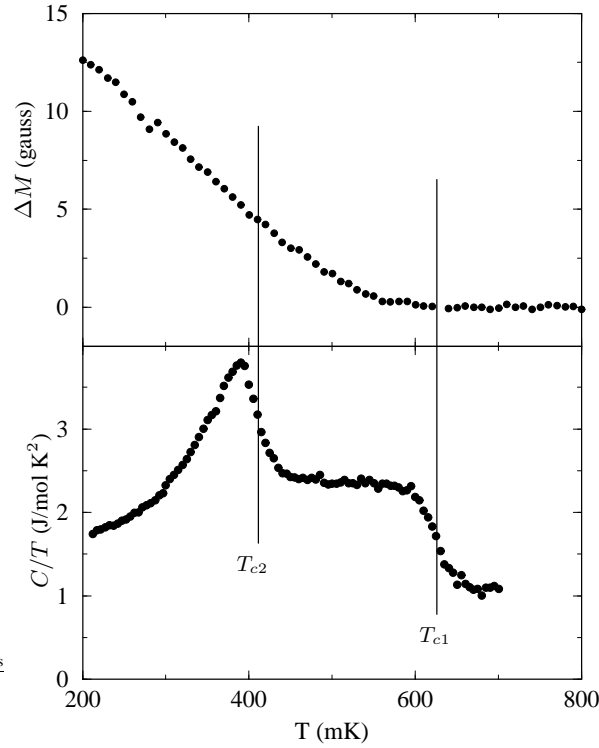


FIG. 3: Comparison of magnetization and heat capacity for unirradiated $\text{U}_{0.97}\text{Th}_{0.03}\text{Be}_{13}$. The vertical lines mark the two transitions.

can change by up to a factor of 5 even for a single sample between cooldowns. This probably happens because the exact location of the gaussmeter changes. Since the samples are polycrystalline, the relevant region for a Bean-type magnetization profile may be a single grain rather than the entire sample. This adds small-scale structure to the magnetization, and means that small changes in gaussmeter position can produce significant changes in the measured hysteresis loops. Since the typical grain dimension of $100 \mu\text{m}$ is significantly larger than the gaussmeter size, we do not consider the effects of having the probe over a grain boundary.

We note that $\Delta M(T)$ in Figure 3 shows no feature at the lower transition. By contrast, magnetic relaxation measurements show a sharp drop in the vortex creep rate at the lower transition [6]. UPt_3 , the other HF compound with two transitions, shows the same behavior: a drop in the relaxation rate at the lower transition [6], but no feature in the magnetization itself [29]. One explanation of the difference between the two measurements is that the mechanism of vortex motion changes at the lower transition, while the pinning strength itself undergoes no sharp change. However, another possibility lies in the magnetic field history of the relaxation measurements. Vortex creep is only suppressed when the sample is exposed to a sufficiently large magnetic field, typically 1 kOe, before having the field reduced to zero for the relaxation measurements [30]. Our hysteresis loops, with maximum width of 200 Oe, may simply be in a different regime where the vortex creep shows no signature at the lower transition.

In other superconductors columnar defects are strong pinning centers, with particularly large effects from commensurability near integral multiples of B_Φ . In our measurements, increased pinning would appear as wider hysteresis loops. However, our loop widths are comparable for unirradiated and irradiated samples. In addition, our hysteresis loops have no features at all, as shown in Figure 4 for the 0.1 T irradiated UBe_{13} crystal. One possibility is that our defects are too much smaller than 100 \AA , the superconducting coherence length [14], to pin vortices. The lack of pinning again suggests that the columnar defects are either not present or far smaller than expected.

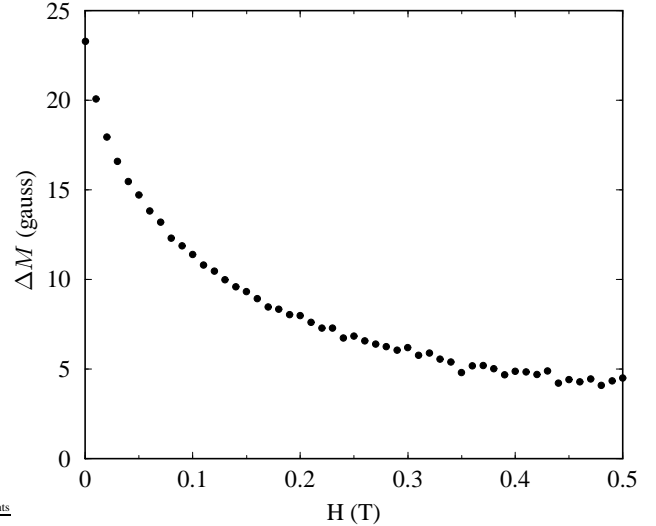


FIG. 4: Hysteresis loop width at 200 mK for pure UBe_{13} with $B_\phi = 0.1$ Tesla.

Our magnetization measurements do show evidence of defect creation. Figure 5 shows loop width versus normalized temperature for $(\text{U,Th})\text{Be}_{13}$ crystals of several irradiation doses, taken at zero nominal field. The width follows a power law $\Delta M(T) = \Delta M(0)(1 - \frac{T}{T_c})^\alpha$ over the entire temperature range measured, approximately $0.3T_c$ to T_c . For the unirradiated and the 5 T samples $\alpha = 1.8$, while for the 7 T specimen α is reduced to 1.4. Although the magnitude agreement between the 5 T and unirradiated samples is partly coincidental, the 7 T sample has significantly the smallest ΔM observed. Both the magnitude and slope change are probably due to the damage. As with the stronger T_c suppression in the 7 T sample mentioned earlier, this hints that the 5 T irradiation is a threshold for strong damage in our $(\text{U,Th})\text{Be}_{13}$ crystals.

Models for networks of superconducting grains give $\alpha = 1$ for superconductor-insulator-superconductor (SIS) tunnel junctions [31] and $\alpha = 2$ for superconductor-normal-superconductor (SNS) junctions [32]. An intermediate power law for $j_c(T)$, with α near 1.5, has been measured in various materials, including the HF material CeCu_2Si_2 [33]. The intermediate values may come from mixtures of SIS and SNS junctions in the samples. Similarly, the change in exponent for our 7 T sample is consistent with irradiation damage chang-

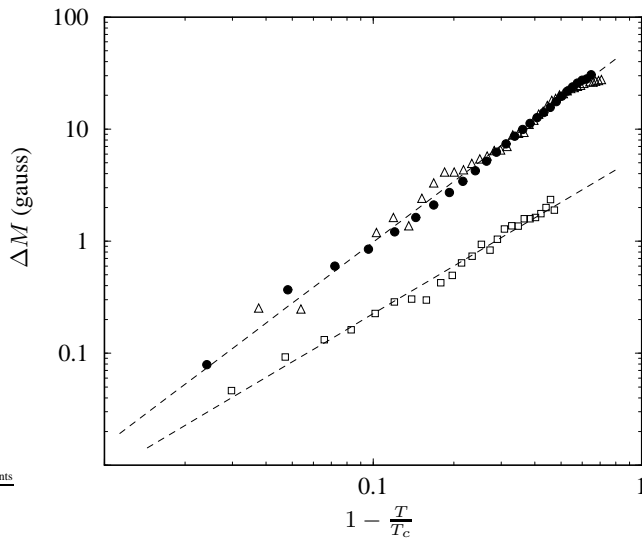


FIG. 5: Hysteresis loop width vs. reduced temperature for three thoriated samples: unirradiated (●), and irradiated with matching fields of 5 T (△) and 7 T (□).

ing the characteristics of the grain network. We find the same power-law behavior in external magnetic fields up to $\mu_0 H = 2$ kG, with the exponent independent of field.

VII. CONCLUSION

We have irradiated (U,Th)Be₁₃ crystals with high-energy U and Pb ions at fluences up to $B_\Phi = 7$ T. The irradiation damage reduces both superconducting transition temperatures of U_{0.97}Th_{0.03}Be₁₃ by over 15% for the 7 T bombardment, as well as lowering j_c and reducing its temperature dependence. Unlike in previous work with substitutional impurities [24], irradiation causes a similar T_c reduction for the two transitions

of U_{0.97}Th_{0.03}Be₁₃.

Despite the measured T_c reduction, transmission electron microscope and hysteresis measurements suggest that the defects are not the amorphous tracks found in HTS. Our calculations of the irradiation process predict columnar defect formation for S_e down to 23 keV/nm. Our samples are irradiated above the threshold value, at $S_e \approx 30$ keV/nm. The resulting defects should have diameter 5 to 6 nm, a defect size comparable to the 10 nm superconducting coherence length. The lack of pinning by the defects and their absence from the TEM images means either that the actual radius is much smaller or that only incomplete columns form. We favor the latter option, based on the similarity between ²⁰⁸Pb⁵⁶⁺ and ²³⁸U⁶⁷⁺ irradiation. If the columns were much smaller for ²³⁸U⁶⁷⁺ ions, they should not appear at all for ²⁰⁸Pb⁵⁶⁺ ions. It is unclear whether the discrepancy with the thermal spike calculation comes from the values chosen for the parameters or from a deeper problem with the model. The conditions for creation of columnar defects are important to understand, particularly as the use of such defects spreads from HTS to other materials.

We also show that the lower transition of U_{0.97}Th_{0.03}Be₁₃ is not detectable in $j_c(T)$, despite the sharp change in magnetic relaxation rate previously observed. This may arise from differences in measurement procedure between our work and the relaxation rate studies. Another possibility is that vortices in the two superconducting phases of U_{0.97}Th_{0.03}Be₁₃ differ only in their behavior away from the critical current j_c , which magnetization measurements would not probe.

VIII. ACKNOWLEDGEMENTS

We would like to thank P.C. Canfield and J.L. Smith for fruitful discussions. This work was supported by NSF under DMR-9733898 (UCD) and by DOE under W-31-109-ENG-38 (ANL), DE-FG05-86ER45268 (Florida), and W-7405-ENG-36 (LANL).

-
- [1] H.R. Ott, H. Rudigier, Z. Fisk, and J.L. Smith, "Phase transition in the superconducting state of U_{1-x}Th_xBe₁₃ ($x = 0$ -0.06)," *Phys. Rev.* **B31**, 1651 (1985).
- [2] R.H. Heffner et al., "New phase diagram for (U,Th)Be₁₃: A muon-spin resonance and H_{c1} study," *Phys. Rev. Lett.* **65**, 2816 (1990).
- [3] B. Andraka et al., "Neutron irradiation of heavy-fermion superconductors," *Phys. Rev.* **B38**, 6402 (1988).
- [4] E.T. Ahrens et al., "NMR study of U(Be,B)₁₃ in the normal and superconducting states," *Phys. Rev.* **B59**, 1432 (1999).
- [5] R.A. Fisher et al., "Specific heat of UPt₃: Evidence for unconventional superconductivity," *Phys. Rev. Lett.* **62**, 1411 (1989).
- [6] A.C. Mota, E. Dumont, and J.L. Smith, "Strong vortex pinning in the low-temperature superconducting phase of (U_{1-x}Th_x)Be₁₃," *J. Low Temp. Phys.* **117**, 1477 (1999); cond-mat/0001185.
- [7] R.J. Zieve et al., "Anomalous flux pinning in a torus of thoriated UBe₁₃," *Phys. Rev.* **B51**, 12041 (1995).
- [8] Z.G. Wang, C. Dufour, E. Paumier, and M. Toulemonde, "The S_e sensitivity of metals under swift-heavy-ion irradiation: A transient thermal process," *J. Phys. Cond. Mat.* **6**, 6733 (1994).
- [9] M. Ghidini et al., "Amorphization of rare earth-cobalt intermetallic alloys by swift heavy-ion irradiation," *J. Phys. Cond. Mat.* **8**, 8191 (1996).
- [10] J.-P. Nozieres et al., "Swift heavy ions for magnetic nanostructures," *Nucl. Instr. Meth.* **B146**, 250 (1998).
- [11] M.P.R. Waligórska, R.N. Hamm, and R. Katz, "The radial distribution of dose around the path of a heavy ion in liquid water," *Nucl. Tracks Radiat. Meas.* **11**, 309 (1986).
- [12] G.R. Stewart, "Heavy-fermion systems," *Rev. Mod. Phys.* **56**, 755 (1984).
- [13] R. Hultgren et al., *Selected Values of the Thermodynamic Properties of Binary Alloys*, (American Society for Metals, Metals Park, OH, 1973).
- [14] R.H. Heffner and M.R. Norman, "Heavy fermion superconductivity," *Comments Cond. Mat. Phys.* **17**, 361 (1996); cond-

- mat/9506043.
- [15] M.W. McElfresh et al., "Structure of the heavy-fermion superconductor UBe_{13} ," *Acta Cryst. C* **46**, 1579 (1990).
- [16] F.G. Aliev et al., "Anisotropy of the upper critical field near T_c and the properties of URu_2Si_2 and UBe_{13} in the normal state," *J. Low Temp. Phys.* **85**, 359 (1991).
- [17] J.S. Kim, B. Andraka, and G.R. Stewart, "Investigation of the second transition in $U_{1-x}Th_xBe_{13}$," *Phys. Rev. B* **44**, 6921 (1991).
- [18] J.F. Ziegler, "The stopping and range of ions in matter (SRIM)," IBM-Research, <http://www.research.ibm.com/ionbeams/>.
- [19] H.A. Radovan et al., "Reduction of critical temperatures in pure and thoriated UBe_{13} by columnar defects," *Physica C* **341-348**, 1953 (2000), cond-mat/9912398.
- [20] L.M. Paulius et al., "Effects of 1-GeV uranium ion irradiation on vortex pinning in single crystals of the high-temperature superconductor $YBa_2Cu_3O_{7-\delta}$," *Phys. Rev. B* **56**, 913 (1997).
- [21] J.T. Kim et al., "Pinning effect on fluctuation conductivity in a superconducting untwinned $YBa_2Cu_3O_{7-\delta}$ single crystal with columnar defects," *Phys. Rev. B* **57**, 7499 (1998).
- [22] A.V. Samoilov et al., "Mixed-state hall conductivity in high- T_c superconductors: Direct evidence of its independence on disorder," *Phys. Rev. Lett.* **74**, 2351 (1995).
- [23] W.-K. Kwok et al., "Anisotropically splayed and columnar defects in untwinned $YBa_2Cu_3O_{7-\delta}$," *Phys. Rev. B* **58**, 14594 (1998).
- [24] E.-W. Scheidt, T. Schreiner, and G.R. Stewart, "Influence of La and Gd impurities on the two phase transitions in $U_{0.97}Th_{0.03}Be_{13}$," *J. Low Temp. Phys.* **114**, 151 (1999).
- [25] G. Adrian and H. Adrian, "Lattice disorder effects on superconductivity and electrical resistivity of heavy-fermion $CeCu_2Si_2$ -films," *Europhys. Lett.* **3**, 819 (1987).
- [26] T. Wiss et al., "Radiation damage in UO_2 by swift heavy ions," *Nucl. Instr. and Meth. B* **122**, 583 (1997).
- [27] A. Berthelot et al., "Irradiation of a tin oxide nanometric powder with swift heavy ions," *Nucl. Instr. and Meth. B* **166-167**, 927 (2000).
- [28] N. Kuroda et al., "Effects of defect morphology on the properties of the vortex system in $Bi_2Sr_2CaCu_2O_{8+\delta}$ irradiated with heavy ions," *Phys. Rev. B* **63**, 224502 (2001).
- [29] E. Shung, T.F. Rosenbaum, and M. Sigrist, "Vortex pinning and stability in the low field, superconducting phases of UPt_3 ," *Phys. Rev. Lett.* **80**, 1078 (1998).
- [30] A.C. Mota, E. Dumont, J.L. Smith, and Y. Maeno, "Unconventional strong pinning in multiphase superconductors," *Physica C* **332**, 272 (2000).
- [31] V. Ambegaokar and A. Baratoff, "Tunneling between superconductors," *Phys. Rev. Lett.* **10**, 486 (1963) and *Phys. Rev. Lett. Erratum* **11**, 104 (1963).
- [32] P.G. de Gennes, "Boundary effects in superconductors," *Rev. Mod. Phys.* **36**, 225 (1964).
- [33] A. Pollini et al., "Flux dynamics and low-field magnetic properties of the heavy-fermion superconductor $CeCu_2Si_2$," *J. Low Temp. Phys.* **90**, 15 (1993).